Int. J. Chem. Sci.: 14(1), 2016, 67-87
ISSN 0972-768X
www.sadgurupublications.com

THEORETICAL STUDY OF STABILITY, MOLECULAR STRUCTURE AND INTRAMOLECULAR HYDROGEN BONDING OF AN ENERGETIC MOLECULE 1-PHENYL-2-NITROGUANIDINE: A QTAIM APPROACH

C. THEIVARASU[a] and RANGASWAMY MURUGESAN[*]

Directorate General of Quality Assurance, Ministry of Defence, CQAFE, PUNE – 411027 (T.N.) INDIA
[a]PSG College of Technology, COIMBATORE – 641004 (T.N.) INDIA

ABSTRACT

In the present work, *ab initio* and density functional theory (DFT) calculations are carried out on the energetic molecule 1-phenyl-2-nitroguanidine to understand its bond topology and its energetic properties using Bader's atoms in molecules (AIM) theory. The optimized geometry predicts that the molecular structure of the compound is nonplanar, but contains two almost planar fragments: nitroguanyl group and phenyl group. The B3LYP/6-31G (d,p) theoretical level predicts that the electron density $\rho(r)$ at the bond critical point of phenyl C-N bond is smaller than that of C-N bonds in nitroguanyl group. Based on the magnitude and sign of the Laplacian $\nabla^2 \rho(r)$ and electron energy density $h_e(r)$ at the critical points of bonds, the interactions are classified as covalent type of interaction in terms of atoms in molecules theory. The energy of the hydrogen bond is evaluated using the Espinoza's formula. The electron energy density $h_e(r)$ and $-g(r)/v(r)$ value of hydrogen bond confirm the partly covalent nature of hydrogen bond. The impact sensitivity (90.5 cm) and oxygen balance (– 9.99%) were calculated and compared with energetic molecules. Large negative electrostatic potential regions were found near the nitro groups where reaction is expected to occur. The stability of compound was considered based on the values of the bond ellipticity and ESP.

Key words: Energetic molecule, Electron density, Laplacian of electron density, Oxygen balance, Hydrogen bond, ESP.

INTRODUCTION

The process of synthesizing energetic materials and qualifying them for military use is not straightforward. It can be tedious, expensive and hazardous. In recent years, significant effort has been made to design new energetic materials with low signature and

[*]Author for correspondence; E-mail: murugeshdenalai@gmail.com

low sensitivity and large number of nitro derivatives have been studied[1-8]. Nitrimines are compounds containing an explosophore group >C=N–NO_2. They are of interest for practical use as energetic substances[9-14]. Nitroguanidine, a well known nitrimine, has been identified as a useful component of gunpowders, solid rocket propellants, and explosive composites. Quantum-chemical methods are not widely used for studying the molecular and electronic structure of these compounds, except 2-nitroguanidine, for which structural analysis has been discussed in the literature for nearly five decades[15-21]. The aim of this work is to compare the experimental and calculated geometrical parameters, bond length, bond angle and QTAIM studies of the molecules; to establish the molecular structure, reactivity and stability of the compound. This allows to estimate the potential of modern computer techniques[22] in predicting the properties of nitrimines, seek quantitative relationships between structure and property, and make forecasts to find new hypothetical energetic nitrimine structures with the desired sets of characteristics. Nitroguanidine and its monosubstituted derivatives generally have a similar structure. The common features are the near-planar geometry of the nitroguanyl group with delocalized π-electron density and bond lengths intermediate between the values characteristic of the typical C–N, N–N and N–O single and double bonds.

Another important characteristic feature of the nitrimine structure is intramolecular hydrogen bond, which stabilizes the planar geometry of the nitroguanyl group. Due to the electron density redistribution, the formally double bond C=NNO_2 is actually not a double bond, nor the shortest C–N bond in nitroguanidines[23-31].

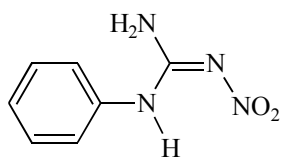

Fig. 1: Chemical structure of 1-phenyl-2-nitroguanidine

Calculation method

Quantum-chemical calculations were carried out by *ab initio* and DFT methods using the GAUSSIAN 03 program[32]. For *ab initio* calculations in the Hartree-Fock (HF) self-consistent field approximation, the 3-21G, 6-31G, 6-311G, 6-311G (d,p) basis sets,[33] have been used and in density functional theory (DFT) with B3LYP[34-35], 6-31G, 6-311G, 6-311G** basis sets have been used and semiempirical calculations were performed in AM1, PM3 and PM6 approximations[36-37]. In the calculation of the IR spectra of the considered structure, all vibrational modes are real indicating the presence of the local energy minima of

the molecule.

A complete analysis was performed on the electron density distribution function ρ(r) for the equilibrium geometry of the compound in the framework of the Bader atoms in molecular theory[38-40]. The topological analysis of the distribution function of the electron density ρ(r) was carried out using the multifunctional wavefunction analysis program in the framework of Multiwfn 3.2.1 software package[41].

The AIM theory: Fundamentals and applications

In modern quantum chemistry, Bader's atoms in molecules (AIM) theory is a powerful tool for predicting the properties and reactivities of the molecular structures. The distribution function of the electron density ρ(r) is a key concept in the AIM theory. The electron density ρ(r) function can be obtained theoretically using quantum chemical calculations and experimentally by the precision X-ray diffraction studies[42].

Bader has shown[38] that molecular structure of a given polyatomic system can be uniquely determined by the function ρ(r) and several other critical points of electron density of the system where the ρ(r) gradient in the critical point is zero. The type and properties of a critical point are defined by the number and sign of the nonzero Eigenvalues λ_i of the Hessian in a critical point, also referred to as the ρ(r) curvature in the critical point. In general, the type of critical point has the form (ω, σ), where ω is the Hessian matrix rank, σ is the signature, that is, the sum of signs of the λ[38]. Bader has shown that the Hessian rank ω at a critical point for equilibrium and energetically stable molecular system is equal to 3 (λ_1, λ_2, $\lambda_3 \neq 0$). When ω = 3, the signature (σ) can have four different values: –3, –1, +1, +3. Accordingly, Bader has stated four types of the critical points, which precisely describe any molecular system:

(i) Critical point (3, –3) corresponds to the position of the atomic nucleus in the space ($\lambda_1, \lambda_2, \lambda_3 < 0$);

(ii) Critical point (3, +1) corresponds to the formation of a ring ($\lambda_1 < 0, \lambda_2, \lambda_3 > 0$);

(iii) Critical point (3, +3) corresponds to the formation of polyhedral (cellular) structure ($\lambda_1, \lambda_2, \lambda_3 > 0$);

(iv) Critical point (3, –1) is an indicator (a necessary and sufficient condition) for the bonding interactions ($\lambda_1, \lambda_2 < 0, \lambda_3 > 0$).

Each type of critical point described above is identified with an element of chemical structure: (3, –3) nuclear critical point (NCP); (3, –1) bond critical point (BCP); (3, +1) ring

critical point (RCP); and (3, +3) cage critical point (CCP). Bond critical point (BCP) plays a key role in describing the molecular structure and enhances the possiblity to establish the existence of binding between the atoms through valence bonds and non-valence interactions.

The number and type of critical points that may exist in the final molecular structure are subjected to the Poincare–Hopf relation[38]:

$$n - b + r - c = 1 \quad \ldots(1)$$

where n is the number of nuclei (nuclear critical point), b is the number of bonding routes (bond critical point), r is the number of rings (ring critical point), and c is the number of cells (cage critical point).

The ratio of λ_1/λ_3 qualitatively describes the type of the corresponding chemical bond[38,43]. When $|\lambda_1/\lambda_3| > 1$ the electron density is concentrated in the interatomic space, which corresponds to a covalent type of interaction. When $|\lambda_1/\lambda_3| < 1$, the electron density is concentrated in the atomic space, which corresponds to the interaction of closed shells (hydrogen, van der Walls, and ionic bonds).

Bader and colleagues have suggested the ellipticity (ε)[44] measures the extent to which density is preferentially accumulated in a given plane containing the bond path. The ellipticity is defined as:

$$\varepsilon = \frac{\lambda_1}{\lambda_2} - 1 \quad (\text{where } |\lambda_1| \geq |\lambda_2|) \quad \ldots(2)$$

Ellipticity is a quantitative description of the deviation of electron density distribution in the critical point (3, –1) from the cylindrical symmetry. The magnitude of ε is a measure of the π-character of the bond. In addition, ε characterizes the susceptibility of a bond in a ring to cleavage, that is, the ring strain.

An important characteristic of bonding interaction is the magnitude and sign of the electron density Laplacian $\nabla^2 \rho(r)$ in the BCP. The magnitude of $\nabla^2\rho(r)$ in the critical point is a measure of the concentration of electron density in the interatomic space and it can be calculated as a sum of the curvature $\rho(r)$ components in the critical point, $\nabla^2\rho(r) = \lambda_1 + \lambda_2 + \lambda_3$.

The classification of interatomic interactions according to the criterion of $|\lambda_1/\lambda_3|$ magnitude and the Laplacian sign[43] does not explain the existence of an intermediate type of

interactions. In intermediate type of interactions, the electron density is largely concentrated in the interatomic space as in the case of covalent bond, but $\nabla^2 \rho(r) > 0$, which is typical for the interaction of closed shells. These interactions particularly comprises of strong polar covalent bonds, coordination bonds, strong hydrogen bonds, and other interactions. To include these interactions in a system of classification of interatomic contacts, Kremer and Kraka proposed a qualitative criterion for describing the interatomic interactions on the basis of the sign of Laplacian and the sign of the electron energy density $h_e(r)$:

$$h_e(r) = g(r) + v(r) \quad \ldots(3)$$

where $g(r)$ is the kinetic energy density in critical point (3, –1), $v(r)$ is the density of potential energy in the critical point (3, –1). The value of ν(r) is always negative by definition, whereas g(r) is always positive. For nonpolar and weakly polar covalent bonds $\nabla^2\rho(r) < 0$ and $| v(r) | > g(r)$, and therefore, $h_e(r) < 0$. For the intermediate type of interactions $\nabla^2\rho(r) > 0$, but $|v(r) | > g(r)$, and therefore $h_e(r) < 0$. For the interaction of the closed shells $\nabla^2\rho(r) > 0$, and $|v(r) | < g(r)$, that is, $h_e(r) > 0$.

An important characteristic of a bond in terms of the AIM theory is the index of delocalization of electron density (DI) between the interacting atoms, which indicates the number of electrons in the interatomic space[38]. Index of delocalization of electron density within the AIM theory is obtained by integrating the density of the Fermi hole. The value of DI can be directly interpreted as the bond order[45].

By analogy with the index of the electron density delocalization, in the AIM theory the index of the electron density localization is also used. Its magnitude indicates the number of electrons (taking into account also the core electrons) localized in the atomic space[38]. At 100% electron localization in atomic space, the Fermi hole of this electron is completely included in the same space.

An important advantage of the AIM theory is the ability to estimate the energy of intra- and intermolecular interactions on the basis of Espinosa correlation[46]:

$$E_{[au]} = 1/2v(r) \sim E_{[kcal/mol]} = 313.754v(r) \quad \ldots(4)$$

where E is the energy of interatomic interaction (au or kcal mol^{-1}). This relationship links the energy of interaction with the potential energy density in the corresponding critical point. It was originally used for finding the hydrogen bonding energy. One of the most important features of intramolecular H-bond is its strength. The intramolecular hydrogen

bonding energy plays a significant role in conformational preference and its value mainly depends on the choice of the resonance state. Many authors have devised various methods to estimate the energy of intramolecular hydrogen bonding. In Shuster method[47], it is assumed that the energy difference between the close (with HB) and open (without HB) conformers is equal to hydrogen bonding energy. But this energy gap also contains some conformational contributions and is not a direct measure of the hydrogen bonding energy. However, in a series of recent papers, the application of the Espinosa formula for determining the energy of coordination[48-49] and homopolar bonds[50] corresponding to an intermediate type of interaction has been expanded.

RESULTS AND DISCUSSION

Molecular geometry and electronic structure

Figure 2 shows the optimized structure of 1-phenyl-2-nitroguanidine calculated at DFT/6-311G** level. The optimized structure exhibits that the compound is nonplanar, but contains almost planar fragments: nitrogunayl and phenyl groups. The values of calculated and experimental bond lengths and angles[51] are listed in Tables 1 and 2. The parameters of bonds involving hydrogen atoms are not listed because the accuracy in determining the positions of hydrogen atoms in XRD analysis is not desirable by order of magnitude.

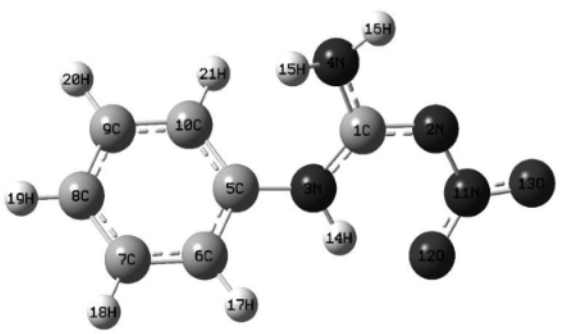

Fig. 2: Optimized structure of 1-phenyl-2-nitroguanidine at DFT/6-311G level**

Among the several methods used, HF/6-31G gave the geometrical parameters that agreed most closely with experimental data. The use of polarization functions and DFT methods did not decrease the deviations; on the contrary, distressing results were obtained. The discrepancy between the calculated and experimental data is due to various factors[52]. One of the most important factors is that XRD data refers to the crystalline substance, while the calculations were performed for the isolated molecule by ignoring intermolecular interactions in the crystal lattice.

Table 1: Experimental and calculated bond lengths (Å) of 1-phenyl-2-nitro guanidine molecule

Bond	Exp.	AM1	PM3	PM6	HF				B3LYP		
					3-21G	6-31G	6-311G	6-311G**	6-31G	6-311G	6-311G**
N(11)-N(2)	1.336	1.368	1.394	1.371	1.372	1.341	1.344	1.345	1.379	1.380	1.371
N(2)- C(1)	1.360	1.373	1.356	1.368	1.357	1.365	1.367	1.318	1.352	1.354	1.334
C(1)-N(3)	1.323	1.397	1.408	1.392	1.335	1.338	1.339	1.334	1.356	1.354	1.347
C(1)- N(4)	1.321	1.385	1.387	1.384	1.328	1.329	1.340	1.339	1.357	1.356	1.352
N(3)-C(5)	1.430	1.414	1.451	1.441	1.430	1.431	1.430	1.427	1.438	1.437	1.430
C(5)-C(6)	1.372	1.411	1.398	1.404	1.384	1.384	1.387	1.386	1.403	1.400	1.397
C(6)-C(7)	1.392	1.392	1.390	1.396	1.383	1.387	1.386	1.384	1.399	1.397	1.392
C(7)-C(8)	1.361	1.394	1.391	1.398	1.364	1.368	1.377	1.384	1.400	1.397	1.393
C(8)-C(9)	1.364	1.394	1.391	1.398	1.369	1.370	1.387	1.384	1.400	1.397	1.393
C(9)-C(10)	1.380	1.392	1.390	1.396	1.383	1.384	1.386	1.384	1.399	1.397	1.392
C(10)-C(5)	1.380	1.410	1.398	1.404	1.38	1.383	1.387	1.386	1.403	1.400	1.397
N(11)-O(12)	1.250	1.219	1.232	1.243	1.290	1.261	1.262	1.212	1.300	1.303	1.254
N(11)-O(13)	1.231	1.202	1.202	1.208	1.227	1.235	1.216	1.178	1.254	1.256	1.216

Table 2: Experimental and calculated bond angles (deg) of 1-phenyl-2-nitro guanidine molecule

Bond	Exp.	AM1	PM3	PM6	HF				B3LYP		
					3-21G	6-31G	6-311G	6-311G**	6-31G	6-311G	6-311G**
O(13)-N(11)-O(12)	120.6	120.916	124.118	124.907	122.205	121.871	121.814	122.779	121.802	121.751	122.398
O(13)-N(11)-N(2)	115.6	116.011	117.526	116.241	115.527	116.342	116.333	115.315	115.913	115.981	115.352
O(12)-N(11)-N(2)	123.8	123.056	118.352	118.852	122.268	121.787	121.853	121.907	122.281	122.267	122.247
C(5)-C(10)-C(9)	119.4	119.976	119.378	118.989	119.928	119.768	119.836	119.849	119.771	119.806	119.868
C(10)-C(9)-C(8)	120.5	120.602	120.339	120.423	120.069	120.067	120.072	120.093	120.139	120.128	120.138
C(9)-C(8)-C(7)	120.0	119.734	120.094	120.075	119.949	120.049	119.994	119.975	120.012	119.993	119.977
C(8)-C(7)-C(6)	120.8	120.558	120.279	120.411	120.084	120.066	120.072	120.092	120.139	120.128	120.138
C(7)-C(6)-C(5)	118.9	120.011	119.441	119.006	119.936	119.768	119.835	119.849	119.770	119.806	119.868
N(3)-C(5)-C(10)	120.8	120.932	119.513	120.172	120.150	119.851	119.896	119.919	119.909	119.925	119.989
N(3)-C(5)-C(6)	118.7	119.879	119.923	118.693	119.808	119.852	119.897	119.920	119.908	119.925	119.989
C(10)-C(5)-C(6)	120.4	119.114	120.462	121.092	120.031	120.281	120.191	120.143	120.169	120.139	120.012
C(5)-N(3)-C(1)	125.3	123.586	120.261	124.968	124.256	124.869	124.689	124.714	124.628	124.633	124.706
N(11)-N(2)-C(1)	119.9	124.049	123.941	124.335	119.551	121.402	121.044	120.471	119.615	119.533	119.522
N(3)-C(1)-N(2)	126.4	125.948	124.213	125.104	127.513	128.195	128.348	128.860	127.534	127.622	127.843
N(3)-C(1)-N(4)	120.7	119.342	122.535	120.456	118.637	118.828	118.802	118.037	118.925	118.966	118.389
N(2)-C(1)-N(4)	112.9	114.679	113.237	114.439	113.849	112.977	112.851	113.103	113.541	113.412	113.768

Therefore, the calculated values, should be compared with the data obtained through gas-phase methods (gas-phase electron diffraction, microwave spectroscopy), but not with XRD parameters. In contrast to X-ray data, gas-phase data on the structures of molecules of energetic compounds are inadequate. For nitrimines, these data are unavailable at present because some of their physicochemical properties (low vapor elasticity and high thermal decomposition rate in both the gas and condensed phases at evaporation or sublimation points) hinder the use of the above methods.

The C–N, N–N, and N–O bonds in the nitroguanyl of the compound have the lengths intermediate between the values typical of the respective single and double bonds in other nitrimines, which indicate the delocalization of p electron density. The geometrical parameters of several nitramines in the gas phase and crystalline state were compared in and for the hexogen molecule in the gas phase, all bond lengths are larger. For C–N and N–O bonds, the difference is insignificant but the difference in the N–N bond lengths is more pronounced (0.033 Å; the error is 0.005 Å).

The average experimental C–C bond length is 1.375 Å in the phenyl group, which is less than that in other aromatic compounds[25], e.g., in nitrobenzene this value is 1.390 Å. The C–C bond lengths vary in a wide range from 1.368 Å for the C(4)–C(5) bond to 1.387 Å for the C(3)–C(4) bond in the phenyl group. Another important aspect is the absence of geometrical symmetry in the phenyl group. This can be caused by the intermolecular interaction.

QTAIM Studies

QTAIM analysis was initiated by searching critical points (CPs). The Poincare-Hopf rule, n-b+r-c = 1, was also tested to ensure the completeness of CP searching and the compound satisfies the rule. According to QTAIM, the bonded atoms are determined by duo-gradient paths of charge density function, which originate from a bond critical point, that is a point, where the gradient of charge density vanishes and the Hessian matrix of charge density has two negative and one positive Eigen-value and terminate on corresponding atomic nuclei. These gradient paths at equilibrium geometry are called “bond paths” which must be regarded as the “Universal indicators of bonded interactions”.

The results of CPs and bond paths searching are gathered in Tables 3, and 4. The quantum mechanical structure is proposed by molecular graph (MG), which is the collection of BCPs and their associated bond paths. These 3D MGs are depicted in Fig. 3, in which some of the BPs are not straight lines but they are displaced outward or inward. These behaviors have been related to “ring strain energy” and “resonance stabilization energy” concepts.

Table 3: Values and ratios of the elements of curvature of the function ρ(*r*) in the critical point (3, –1) of the coordination bonds, as well as localization parameters of the electron density in the atomic and interatomic space

Bond	λ1 (a.u)	λ2 (a.u)	λ3 (a.u)	λ1/λ3	ε	ρ(r) (a.u)	∇²ρ(r) (a.u)	DI
C5-C6	-0.5649	-0.4846	0.3872	-1.4587	0.1658	0.2853	-0.6622	1.3242
C6-C7	-0.5609	-0.4923	0.3794	-1.4786	0.1395	0.2864	-0.6738	1.4014
C7-C8	-0.5583	-0.4930	0.3824	-1.4601	0.1325	0.2855	-0.6689	1.3889
C8-C9	-0.5587	-0.4931	0.3823	-1.4613	0.1330	0.2856	-0.6695	1.3904
C9-C10	-0.5579	-0.4902	0.3795	-1.4700	0.1380	0.2856	-0.6686	1.3981
C10-C5	-0.5583	-0.4803	0.3861	-1.4461	0.1625	0.2837	-0.6525	1.3180
N11-O12	-1.0632	-1.0065	1.6523	-0.6435	0.0563	0.4253	-0.4174	1.4772
N11-O13	-1.1607	-1.1003	1.7056	-0.6805	0.0549	0.4557	-0.5554	1.6050
N11-N2	-0.6876	-0.6186	1.0407	-0.6607	0.1117	0.3078	-0.2655	1.1387
N3-C5	-0.4807	-0.4609	0.3584	-1.3412	0.0429	0.2618	-0.5832	0.9823
N2-C1	-0.7199	-0.6337	0.4914	-1.4652	0.1361	0.3329	-0.8622	1.3060
C1-N3	-0.6401	-0.5696	0.4353	-1.4706	0.1239	0.3096	-0.7744	1.1661
C1-N4	-0.6309	-0.5707	0.4596	-1.3729	0.1054	0.3009	-0.7421	0.9488

Table 4: Coordination bond lengths (d), energies (E), and the topological characteristics of the electron density distribution in the critical point (3, –1)

Bond	d1 (Å)	d2 (Å)	D (Å)	v(r) (a.u)	g(r) (a.u)	h(r) (a.u)	E (kJ/Mol)
C5-C6	0.6865	0.7229	1.4093	-0.3534	0.0939	-0.2595	-110.8665
C6-C7	0.7062	0.6970	1.4031	-0.3567	0.0941	-0.2626	-111.9157
C7-C8	0.7053	0.7003	1.4056	-0.3535	0.0931	-0.2603	-110.8975
C8-C9	0.7003	0.7051	1.4054	-0.3538	0.0932	-0.2606	-111.0085
C9-C10	0.6980	0.7064	1.4044	-0.3548	0.0938	-0.2610	-111.3281
C10-C5	0.6857	0.7249	1.4105	-0.3510	0.0939	-0.2571	-110.1189
N11-O12	0.6161	0.6352	1.2513	-0.7312	0.3134	-0.4177	-229.4048
N11-O13	0.6045	0.6213	1.2258	-0.8152	0.3382	-0.4770	-255.7778

Cont…

Bond	d1 (Å)	d2 (Å)	D (Å)	v(r) (a.u)	g(r) (a.u)	h(r) (a.u)	E (kJ/Mol)
N11-N2	0.6596	0.7304	1.3897	-0.4068	0.1702	-0.2366	-127.6301
N3-C5	0.5617	0.8559	1.4175	-0.4191	0.1367	-0.2824	-131.4938
N2-C1	0.7588	0.5742	1.3318	-0.5329	0.1587	-0.3742	-167.2052
C1-N3	0.5605	0.7945	1.3549	-0.5074	0.1569	-0.3505	-159.2114
C1-N4	0.7034	0.3914	1.0948	-0.4499	0.1322	-0.3177	-141.1677

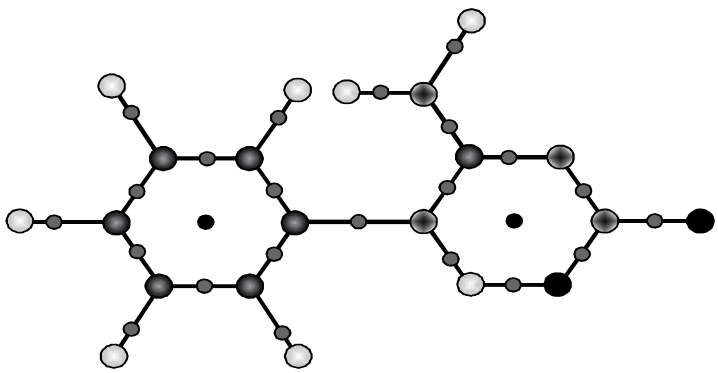

Fig. 3: Complete molecular 3D view at DFT/6-311G: C nucleus: (●) circles; H nucleus: (○) circles; N nucleus: (●) circles; O nucleus: (●) circles; BCP: (●) circles; RCP: (●) circles; Bond paths: (—) lines**

H-bond energies

The large difference between the bond lengths obtained in calculation and experiment (XRD) for 1-phenyl-2-nitroguanidine is attributed to the action of intermolecular interactions, in particular, hydrogen bonds. The optimized structure with hydrogen bonding of 1-phenyl-2-nitroguanidine is shown in Fig. 4.

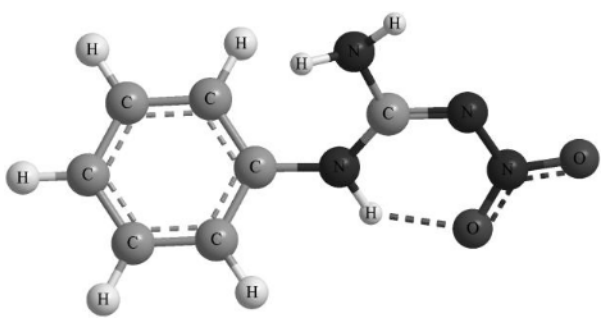

Fig. 4: Optimized structure of 1-phenyl-2-nitroguanidine with hydrogen bonding

As Rozas et al.[53] explained; hydrogen bonds can be classified as follows:

(i) Weak hydrogen bonds of electrostatic character $\nabla^2\rho(r_{BCP}) > 0$ and $g(r_{BCP}) + v(r_{BCP}) > 0$.

(ii) Medium hydrogen bond of partially covalent nature $\nabla^2\rho(r_{BCP}) > 0$ and $g(r_{BCP}) + v(r_{BCP}) < 0$.

(iii) Strong hydrogen bond of covalent nature $\nabla^2\rho(r_{BCP}) < 0$ and $g(r_{BCP}) + v(r_{BCP}) < 0$.

where $g(r_{BCP}) + v(r_{BCP})$ is also known as total electron energy density, $h(r_{BCP})$. The nature of IHB (Intramolecular hydrogen bond) can be determined using ratio of $-g(r_{BCP})/v(r_{BCP})$. The value of $-g(r_{BCP})/ v(r_{BCP}) > 1$ for IHB having noncovalent nature, and $0.5 < -g(r_{BCP})/ v(r_{BCP}) < 1$ for IHB having partly covalent nature. Prediction of IHB energy is one of the most important subjects in recent studies not only for its characterization, but also due to the role, it plays in numerous processes, for example, in hydration. Several theoretical methods have been proposed to estimate hydrogen bond energy. One of the most useful of these methods has been explained by Espinosa et al. who found that IHB energy may be correlated with the potential electron energy density at critical point by the expression $E_{IHB} = 1/2v(r_{BCP})$.

The calculated electron density (ρ) and its second derivative $\nabla^2\rho$ were used for describing the nature of the intramolecular N–H···O bond. The calculated electron density (ρ), its Laplacian $\nabla^2 \rho$ at bond critical points and charge density at ring critical point $\rho_{(RCP)}$, its Laplacian $\nabla^2 \rho_{(RCP)}$ for IHB is given in Table 5. According to this table, IHB under investigation, Laplacian of total electronic density at BCPs is positive and reveal that electronic charge is depleted in the interatomic path, which is characteristic of closed shell interactions. In the last column of Table 5, hydrogen bond energy calculated based on Espinosa's equation is presented. This value also clarifies that IHB interactions investigated in this study can be classified as partly covalent nature. The $-g(r)/v(r)$ value of IHB is nearly unit, which also confirms the partly covalent nature of hydrogen bond.

Table 5: Topological parameters (in a.u.) and IHB energies (kcal/mol) calculated on the B3LYP/6-311G wave functions**

H-Bond	$\rho(r_{BCP})$	$\nabla^2(r_{BCP})$	v(r)	g(r)	−g(r)/v(r)	$\rho(r_{RCP})$	$\nabla^2(r_{RCP})$	E_{IHB}
H14-O12	0.0444	0.1501	-0.0436	0.0431	0.9876	0.0191	0.1106	-13.68

Further, under the AIM framework, Lipkowski et al.[54] proposed three criteria for existence of H-bond: (1) The H-bond must be accompanied by a BCP; (2) ρ at BCP (ρ_{BCP}) should be within 0.002-0.04 a.u.; and (3) $\nabla^2\rho$ at BCP ($\nabla^2\rho_{BCP}$) should between 0.02-0.15. In 1-phenyl-2-nitroguanidine, the BCPs between the hydrogen and the oxygen were successfully located (see Fig. 3) for illustration of their positions. For the titled molecule, ρ_{BCP} and $\nabla^2\rho_{BCP}$ are 0.0444 and 0.1501, respectively; which fully satisfy the Lipkowski's rule, showing very strong evidence of the existence of H-bonds in 1-phenyl-2-nitroguanidine.

Topological analysis

There are several local (i.e., calculated at the BCP) and integral (i.e., calculated over the atomic basin) topological properties of the electron density that have been used to analyze the bonding in molecules of the titled compound. Among the former, the electron density, the ellipticity, the Laplacian of the electron density, λ_1/λ_3 ratio and the h(r) = g(r) + v(r), where v(r) is the potential energy density. On the other hand, the delocalization index (DI), which is an integral property, indicates the number of electron pairs shared by atoms A and B. Values of these topological properties, for selected bonds of titled compound, are collected in Tables 3 and 4.

Generally, in shared interactions the charge density is accumulated between two bonded nuclei and the Laplacian is of the same order of magnitude as the charge density. Usually, in these interactions the Laplacian takes negative values. In accordance with the previous statement, Table 4 shows the negative values of the Laplacian and the electron energy density at the BCP of all the bonds. It was pointed out in earlier studies that the negative value indicates the covalent character of interaction between atoms connected by the corresponding bond path; at least such an interaction is characterized by the partial covalence. i.e., the electron density is largely concentrated in the interatomic space. It is further confirmed from the Table 3, the values of $|\lambda_1/\lambda_3| > 1$ shows that the electron densities of these bonds are concentrated in the interatomic space, which corresponds to a covalent type of interaction.

DFT method predicts a low negative Laplacian value for the N-NO_2 bond i.e. – 0.2655 a.u. The low negative value of the Laplacian indicates that the charge of this bond is highly depleted. The potential energy density v(r) of N-NO_2 band is – 0.4068 a.u. and total energy density h(r) is – 0.2366 a.u. From the bond topological parameters, it is predicted that the N-NO_2 bond is the weakest bond in the molecule. Further, from the Table 3, it is observed that slight changes on bond parameters of C_5-C_6 and even slighter on C_5-C_{10} is observed due to the substitutions at C_5.

The bond ellipticity is the measure of anisotropy of electron density distribution at the BCP of bonds. It can be calculated from equation (2). Here, we found maximum ellipticity for the C–C bonds of the aromatic ring and minimum ellipticity for the N=O bonds whereas C–N bonds shows intermediate bond ellipticity values between C–C bonds and N=O bonds. The order of ellipticity values for the three types of bonds in the molecule is C–C > C–N > N=O. The highest ellipticity, and also the highest delocalization index values that are consistent with a formal double bond with a certain degree of delocalization within the benzene ring. DI results indicate that the N(11)-O(12), N(11)-O(13) and N(2)-C(1) bonds have a slightly greater character of double bonds than the N(3)-C(5), N(4)-C(1) and N(3)-C(1) bonds.

Molecular stability and oxygen balance

The energy gap (ΔE) is one of the most important parameters for predicting the relative stability of compounds. Thus, the highest occupied molecular orbital (HOMO) energy, the lowest unoccupied molecular orbital (LUMO) energy, and the energy gap ($\Delta E_{LUMO–HOMO}$) were calculated at the B3LYP/6-311G (d,p) level. Analysis of the molecular orbital can provide useful information on electronic structures.[55] Fukui et al.[56] have observed for the first time the prominent role played by the highest occupied molecular orbital (HOMO) and the lowest unoccupied molecular orbital (LUMO) in governing the chemical reactions of compounds. The principle of easiest transition (PET) states that the smaller is the band gap ($\Delta E_{LUMO-HOMO}$) between HOMO and LUMO, the easier will be the electron transition and the lesser the stability. The DFT method predicts that the band gap ($\Delta E_{LUMO-HOMO}$) of the 1-phenyl-2-nitroguanidine molecule is 5.2 eV, which is found to be much larger than for the energetic propellant molecules TNB, TNT and TATB, for which the respective values are 5.007, 4.925 and 4.054 eV. This indicates that 1-phenyl-2-nitroguanidine is a very stable molecule (Table 6). Overall, the titled compound is a stable molecule, and the stability here refers to a chemical process with electron transfer or electron excitation in the molecule.

The Oxygen Balance (OB_{100}) is one of the important properties of energetic materials, which can be used to roughly predict the impact sensitivities of the explosives. It is defined as "the amount of oxygen, expressed in weight percent, liberated as a result of complete conversion of the explosive material to carbon dioxide, water, sulfur dioxide, aluminium oxide, etc.[57-59] A positive oxygen balance produces greater quantity of NOx gases and a negative oxygen balance produces CO. The equation for the calculation of oxygen balance (OB) is:

$$OB_{100} = \frac{100\,(2n_O - n_H - 2n_C - 2n_{COO})}{M} \qquad \ldots(5)$$

where n_O, n_H, and n_C represent the number of O, H, and C atoms, respectively; n_{COO} is the number of COO^-, and here $n_{COO} = 0$ for the titled compound, M is the molecular weight.

The calculated oxygen balance of the titled molecule is found to be negative and the value is – 9.99% (Table 6). This value has been compared with other reported explosives having positive oxygen balance (OBs) (HNB ~3.45%, PNA ~ 1.89%) as well as negative OBs (TNT -3.08%; TNB – 1.41%; TATB – 2.33%; RDX – 22%; HMX – 22%).

Table 6: Comparison of the energy gap, oxygen balance (OB%) and H_{50}% of 1-phenyl-2-nitroguanidine with reported explosive molecules

Compound	OB %	HOMO	LUMO	$\Delta E_{LUMO-HOMO}$	H_{50}%
		(eV)	(eV)	(eV)	(cm)
1-Phenyl-2-nitroguanidine	-9.99	-0.247	-0.0588	5.12	90.5
TATB	-2.33	-7.102	-3.292	4.054	320.0
TNB	-1.41	-9.905	-4.898	5.007	149.0
TNT	-3.08	-7.891	-2.099	4.925	160.0
HNB	3.45	-	-	-	10.00
PNA	1.89	-	-	-	14.0

Furthermore, using another statistical quantity associated with the electrostatic potential of the molecule, the balance parameter ν, we have calculated the impact sensitivity of the 1-phenyl-2-nitroguanidine molecule[60]. The following equation was obtained from best fit of data:

$$H_{50}\% = 29.3 + 1.386.10^{-3}\, e^{[48.84.\nu]} \quad \ldots(6)$$

A close inspection of the structural parameters of this equation provides the physical insight into the structure-impact sensitivity relationship. The predicted H_{50}% (2.5 Kg drop mass) value for the 1-phenyl-2-nitroguanidine molecule is 90.5 cm. This lower value would make the compound slightly sensitive to impact.

Molecular electrostatic potential and sensitivity

The theoretical electrostatic potential (ESP) of the compound was computed at the optimized structure at the B3LYP/6-311G (d,p) level of theory. Fig. 5 shows the electrostatic potential for the 0.001 electron/bohr^3 isosurfaces of electron along with surface extrema of

1-phenyl-2-nitroguanidine evaluated at the B3LYP/6-311G(d,p) level of theory. The colors range from – 43.0 to + 47.0 kcal/mole with red denoting extremely electron-deficient regions (*V(r)* > + 47.0 kcal/mole) and dark blue denoting electron-rich regions (*V(r)* < -43.0 kcal/mole). It has been found recently by Murray et al.[61] and extensively used by Rice and Hare[62] that the patterns of the computed electrostatic potential on the surface of molecules can be related to the sensitivity of the bulk material. The electrostatic potential V(r) that is created at any point r in the space around a molecule by its nuclei and electrons is given rigorously by,

$$V(r) = \sum \frac{Z_A}{|R_A - r|} - \int \frac{\rho(r')}{|r' - r|} dr' \quad \ldots(7)$$

Where Z_A is the charge on nucleus A, located at R_A, and ρ(r) is the molecule's electronic density. Murray et al. were able to show[61] that impact sensitivity can be expressed as a function of the extent of this anomalous reversal of the strengths of the positive and negative surface potentials.

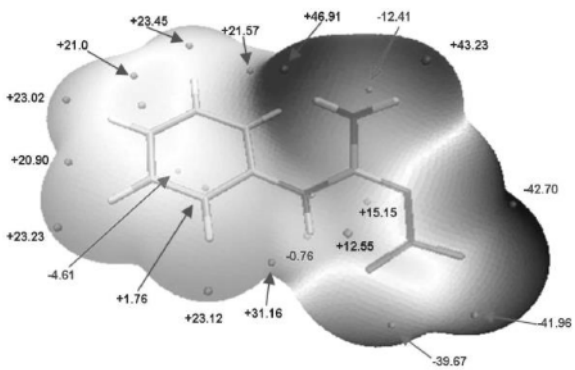

Fig. 5: ESP-mapped molecular surface of 1-phenyl-2-nitroguanidine. The unit is in kcal/mol. Surface local minima and maxima of ESP are represented as green and orange spheres, respectively. The transparent ones correspond to the extrema at backside of graph. The local surface maxima with negative ESP values are meaningless and thus not shown, only the global minimum and maximum are labeled

It is known that the delocalization of π electrons over an aromatic ring is affected by both electron-withdrawing and electron-donating substituents attached to the ring. In their study, Murray et al.[61] found that for the nitroaromatics, the ESP on the surface above the aromatic ring was positive reflecting the electron-withdrawing effect of the nitro groups. The calculated electrostatic potential of the molecule (Fig. 5) reproduces these findings. Electrostatic potential (ESP) on molecular surface is critical for studying and predicting

intermolecular interaction[63]. This parameter can be used to predict the electrophilic and nucleophilic sites in the molecule, where chemical reactions are expected to occur. The map explicitly shows that highly charge-depleted bond is the sensitive bond in the molecule.

Fig. 5 shows that for the lone pair of each oxygen atom leads to one or more ESP minima on the surface, and the value of the most negative one is – 42.70 kcal/mol, which is also the global surface minimum of 1-phenyl-2-nitroguanidine. Each surface maximum in the molecule corresponds to hydrogen, and the global maximum one (46.91 kcal/mol) stems from the prominent positive charge of H15. A large electronegative potential is found in the vicinity of the $–NO_2$ group, and a small electronegative region near the benzene ring atoms.

The graph (Fig. 6) illustrates how the whole 1-phenyl-2-nitroguanidine surface is partitioned. From the graph, it is seen that there is a large portion of molecular surface having small ESP value, namely from – 15 to 25 kcal/mol. Among these areas, the negative part mainly corresponds to the surface above and below the benzene ring and shows the effect of the abundant p-electron cloud, the positive part mainly arises from the positive charged C-H hydrogen. There are small areas having significant negative ESP value, i.e – 20 to – 42.7 kcal/mol, which corresponds to the $–NNO_2$ region and is close to the global ESP minima. There are also small areas having remarkable positive ESP value, corresponding to the regions closed to the global ESP maximum.

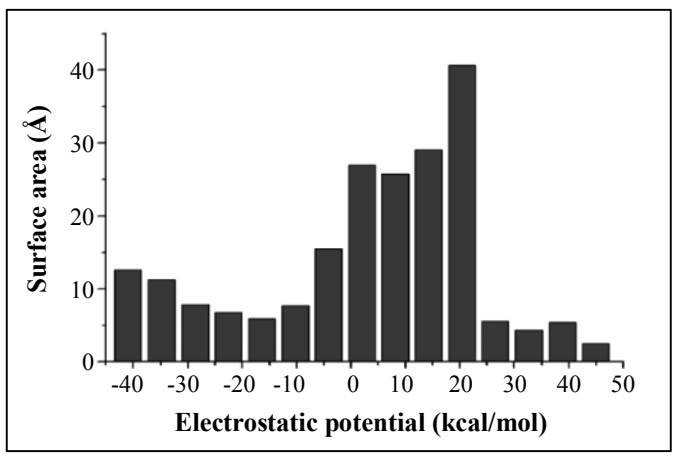

Fig. 6: Surface area in each ESP range on the surface of 1-phenyl-2-nitroguanidine

CONCLUSION

Thus, for evaluating the geometrical parameters and the ensuing properties of nitrimine molecules, one can successfully use *ab initio* calculations at a moderate level with

the 6-31G basis set, which do not require significant effort and are realizable on modern personal computers. The use of additional methods for modeling the crystal packing and the corresponding computing facilities will naturally increase the accuracy of prediction. The bond topological and electrostatic properties of the energetic 1-phenyl-2-nitroguanidine molecule were evaluated by density functional theory at B3LYP/6-311G (d,p) level. From the topological parameters, it is predicted that the N-NO_2 bond is the weakest bond in the molecule compared with all other bonds in the molecule. Compared with other reported explosives, the 1-phenyl-2-nitroguanidine molecule exhibits a wide band gap (5.12 eV) and a negative oxygen balance (– 9.99%). Using the oxygen balance and the nitro group charges, we have calculated the impact sensitivity (H_{50}%) of the 1-phenyl-2-nitroguanidine molecule as 90.5 cm, which makes the compound slightly sensitive to impact. Furthermore, the ESP predicts that a large electronegative potential is found in the vicinity of the –NO_2 group, and a small electronegative region near the benzene ring atoms. The predicted energetic parameters indicate that 1-phenyl-2-nitroguanidine is a potential energetic molecule and hence, further analysis of the derivatives of the 1-phenyl-2-nitroguanidine would be worthful.

REFERENCES

1. R. J. Butcher, J. C. Bottaro and R. Gilardi, Ammonium 1,3,4,6-tetranitro-2,5-diazapentalene, Acta Cryst., **E59**, 1149 (2003).
2. R. J. Butcher, J. C. Bottaro and R. Gilardi, 1-Nitro-7,8-diazapentalene, Acta Cryst., **E59**, 1777 (2003).
3. R. J. Butcher, J. C. Bottaro and R. Gilardi, Potassium 1,3,4,6-tetranitro-2,5-diazapentalene, Acta Cryst., **E59**, 591 (2003).
4. R. J. Butcher, J. C. Bottaro and R. Gilardi, 1,3,4-Trinitro-7,8-diazapentalene, Acta Cryst., **E59**, 1780 (2003).
5. J. S. Muray, P. Lane and P. Politzer, Mol. Phys., **85(1)**, 1 (1995).
6. B. M. Rice and J. J. Hare, J. Phys. Chem. A., **106**, 1770 (2002).
7. J. P. Agrawal, High Energy Materials, Wiley-VCH, Weinheim (2011).
8. T. M. Klapötke, Chemistry of High Energy Materials, Wdeg, Berlin (2011).
9. A. F. McKay, Chem. Rev., **51(2)**, 301 (1952).
10. Y. Yongzhong, S. Zhuang, D. Baoru and C. Fubo, Propellants, Explosives, Pyrotechnics, **14(4)**, 150 (1989).
11. A. M. Astakhov, I. V. Gelemurzina and A. D. Vasiliev, Energetic Materials Ignition, Combustion and Detonation, 32nd Int. ICT Conf., Karlsruhe, FRG, 139/1-10 (2001).

12. E. Yu. Orlova, Chemistry and Technology of Brisant Explosives, Khimiya, Leningrad (1973).

13. R. M. Doherty and R. L. Simpson, Energetic Materials Combustion and Detonation, 28nd Int. ICT Conf., Karlsruhe, FRG, 32/1-23 (1997).

14. A. Maranda, A. Kubecki and J. Nowaczewski, New Trends in Research of Energetic Materials, Proc. 8th Seminar Pardubice, Czech Republic, 665 (2005).

15. A. J. Owen, Tetrahedron, **14(3/4)**, 237 (1961).

16. A. J. Owen, Tetrahedron, **23(4)**, 1857 (1967).

17. J. Stals and M. G. Pitt, Aust. J. Chem., **28(12)**, 2629 (1975).

18. P. Politzer, N. Sukumar, K. Jayasuriya and S. Ranganathan, J. Am. Chem. Soc., **110(11)**, 3425 (1988).

19. R. Caminiti, A. Pieretti and L. Bencivenni, J. Phys. Chem., **100(26)**, 10928 (1996).

20. T. Vladimiroff, Proc. 34th JANN AF Combustion Meeting, 1, 261, CPIA Publication, 662 (1997).

21. A. J. Bracuti, J. Chem. Cryst., **29**, 671 (1999).

22. P. Politzer, J. S. Murray and J. M. Seminario, J. Mol. Struct. (Theochem), **573**, 1 (2001).

23. A. M. Astakhov, A. D. Vassiliev and M. S. Molokeev, Energetic Condensed Systems, Proc. 3rd All-Russian Conf., Chernogolovka, Yanus-K, Moscow, 18/19 (2006).

24. A. M. Astakhov, A. D. Vassiliev, M. S. Molokeev and R. S. Stepanov, Energetic Condensed Systems, Proc. 2nd All-Russian Conf., Chernogolovka, Yanus-K, Moscow, 19/20 (2004).

25. F. H. Allen, Acta Crystallogr., **B58**, 380 (2002).

26. S. Nordenson, Acta Crystallogr., **B37**, 1543 (1981).

27. A. D. Vasiliev, A. M. Astakhov and A. A. Nefedov, Acta Crystallogr., **C57**, 625 (2001).

28. A. D. Vasiliev, A. M. Astakhov and M. S. Molokeev, Acta Crystallogr., **E59**, 193 (2003).

29. A. M. Astakhov, A. D. Vassiliev and M. S. Molokeev, J. Struct. Chem., **44(2)**, 364 (2003).

30. A. M. Astakhov, A. A. Nefedov and A. D. Vasiliev, Energetic Materials Structure and Properties, 35th Int. ICT Conf., Karlsruhe, FRG, P58/1-12 (2004).

31. A. M. Astakhov, A. D. Vassiliev and M. S. Molokeev, Zh. Org. Khim., **41(6)**, 928 (2005).

32. M. J. Frisch, G. W. Trucks, H. B. Schlegel, G. E. Scuseria, M. A. Robb, J. R. Cheeseman, V. G. Zakrzewski, J. A. Montgomery, R. E. Stratmann, J. C. Burant, S. Dapprich, J. M. Millam, A. D. Daniels, K. N. Kudin, M. C. Strain, O. Farkas, J. Tomasi, V. Barone, M. Cossi, R. Cammi, B. Mennucci, C. Pomelli, C. Adamo, S. Clifford, J. Ochterski, G. A. Petersson, P. Y. Ayala, Q. K. Cui, D. K. Morokuma, B. B. Malick Stefanov, G. Liu, A. Liashenko, P. Piskorz, I. Komaromi, R. Gomperts, R. L. Martin, D. J. Fox, T. Keith, M. A. Al-Laham, C. Y. Peng, A. Nanayakkara, C. Gonzalez, M. Challacombe, P. M. W. Gill, B. Johnson, W. Chen, M. W. Wong, J. L. Andres, C. Gonzalez, M. Head-Gordon, E. S. Replogle and J. A. Pople, Gaussian 03, Gaussian Inc., Pittsburgh, PA (2003).

33. J. –Y. Zhang, H.-C. Du, F. Wang, X.-D. Gong and Y.-S. Huang, J. Phys. Chem. A., **115**, 6617 (2011).

34. C. Lee, W. Yang and R. G. Parr, Phys. Rev. B., **37**, 785 (1988).

35. A. D. Becke, J. Chem. Phys., **98**, 5648 (1993).

36. F. Jensen, Introduction to Computional Chemistry, Wiley, New York (2001).

37. J. J. P. Stewart, J. Comp. Chem., **10**, 209 (1989).

38. R. W. F. Bader, Atoms in Molecules, A Quantum Theory, Calendon Press, Oxford (1990).

39. R. F. W. Bader, Acc. Chem. Res., **18(1)**, 9 (1985).

40. R. F. W. Bader, Chem. Rev., **91(5)**, 893 (1991).

41. T. Lu and F. Chen, Multiwfn: A Multifunctional Wavefunction Analyzer, J. Comput. Chem., **33**, 580 (2012).

42. Abramov and A. Yu, Acta Crystallogr. (A), **53(3)**, 264 (1997).

43. R. F. W. Bader and H. Essen, J. Chern. Phys., **80(5)**, 1943 (1984).

44. R. F. W. Bader, T. S. Slee, D. Cremer and E. Kraka, J. Am. Chem. Soc., **105(15)**, 5061 (1983).

45. C. L. Firme, O. A. C. Antunes and P. M. Esteves, Chem. Phys. Lett., **468(4-6)**, 129 (2009).

46. E. Espinosa, E. Molins and C. Lecomte, Chem. Phys. Lett., **285(3-4)**, 170 (1998).

47. P. Schuster, G. Zundel, C. Sandorfy and Amsterdam, The Hydrogen Bond-Recent Developments in Theory and Experiments, Vols. I–III, North Holland (1976).

48. A. O. Borissova, A. A. Korlyukov, M. Yu. Antipin and K. A. Lyssenko, J. Phys. Chem. (A), **112(46)**, 11519 (2008).

49. L. N. Puntus, K. A. Lyssenko, M. Yu. Antipin and J.-C. G. Bünzli, Inorg. Chem., **47(23)**, 11095 (2008).

50. K. A. Lysenko, M. Yu. Antipin and B. H. Khrustalev, Izv. Akad. Nauk, Ser. Khim., **50(9)**, 1465 (2001).

51. A. M. Astakhov, A. D. Vassiliev and V. A. Revenko, J. Struct. Chem., **53(5)**, 1013 (2012).

52. L. A. Gribov, Ross. Khim. Zh., **49(2)**, 137 (2005).

53. I. Rozas, I. Alkorta and J. Elguero., J. Am. Chem. Soc., **122** 11154 (2000).

54. P. Lipkowski, S. J. Grabowski, T. L. Robinson, J. Leszczynski, J. Phys. Chem. A., **108**, 10865 (2004).

55. S. J. Blanksby and G. B. Ellison, Acc. Chem. Res., **36**, 255 (2003).

56. K. Fukui, T. Yonezawa and H. Shingu, J. Chem. Phys., **20**, 722 (1952).

57. V. Thottempudi, H. Gao and J. M. Shreeve, J. Am.Chem. Soc., **133(16)**, 6464 (2011).

58. Y. Liu, X. Gong, L. Wang, G. Wang and H. Xiao, J. Phys. Chem. A., **115(9)**, 1754 (2011).

59. P. Politzer, P. R. Laurence, L. Abrahmsen, B. A. Zilles and P. Sjoberg, Chem. Phys. Lett., **111(1)**, 75 (1984).

60. C. Cao and S. Gao, J. Phys. Chem B., **111**, 12399 (2007).

61. J. S. Murray, P. Lane and P. Politzer, Mol. Phys., **85**, 1 (1995).

62. B. M. Rice and J. J. Hare, J. Phys. Chem., **106A**, 1770 (2002).

63. J. S. Murray and P. Politzer, The Electrostatic Potential: An Overview, Wiley Interdiscip Rev., **(1)**, 153 (2011).

Revised : 22.12.2015 *Accepted : 24.12.2015*